AD-A148 905 RAMAN SIDESCATTERING IN LASER-PRODUCED PLASMAS(U) NAVAL RESEARCH LAB WASHINGTON DC C R MENYUK ET AL. 27 DEC 84 NRL-MR-5483 1/1

UNCLASSIFIED F/G 20/6 NL

END

FILMED

DTIC

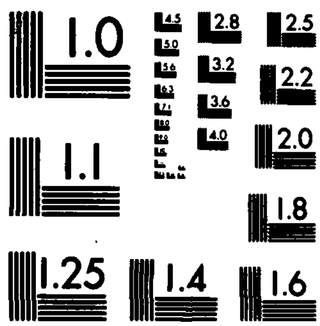

MICROCOPY RESOLUTION TEST CHART
NATIONAL BUREAU OF STANDARDS-1963-A

NRL Memorandum Report 5483

Sidescattering in Laser-Produced Plasmas

C. R. MENYUK AND N. M. EL-SIRAGY

Laboratory for Plasma and Fusion Energy Studies
University of Maryland
College Park, MD 20742

W. M. MANHEIMER

Plasma Theory Branch
Plasma Physics Division

December 27, 1984

NAVAL RESEARCH LABORATORY
Washington, D.C.

AD-A148905

SECURITY CLASSIFICATION OF THIS PAGE

REPORT DOCUMENTATION PAGE

1a. REPORT SECURITY CLASSIFICATION UNCLASSIFIED	1b. RESTRICTIVE MARKINGS
2a. SECURITY CLASSIFICATION AUTHORITY	3. DISTRIBUTION / AVAILABILITY OF REPORT Approved for public release; distribution unlimited.
2b. DECLASSIFICATION / DOWNGRADING SCHEDULE	
4. PERFORMING ORGANIZATION REPORT NUMBER(S) NRL Memorandum Report 5483	5. MONITORING ORGANIZATION REPORT NUMBER(S)
6a. NAME OF PERFORMING ORGANIZATION Naval Research Laboratory — 6b. OFFICE SYMBOL (If applicable) Code 4790	7a. NAME OF MONITORING ORGANIZATION
6c. ADDRESS (City, State, and ZIP Code) Washington, DC 20375-5000	7b. ADDRESS (City, State, and ZIP Code)
8a. NAME OF FUNDING / SPONSORING ORGANIZATION U.S. Department of Energy — 8b. OFFICE SYMBOL (If applicable)	9. PROCUREMENT INSTRUMENT IDENTIFICATION NUMBER
8c. ADDRESS (City, State, and ZIP Code) Washington, DC 20545	10. SOURCE OF FUNDING NUMBERS

PROGRAM ELEMENT NO.	PROJECT NO.	TASK NO.	WORK UNIT ACCESSION NO.
	(See page ii)		DN220-133

11. TITLE (Include Security Classification)

Raman Sidescattering in Laser-Produced Plasmas

12. PERSONAL AUTHOR(S)

Menyuk,* C.R., El-Siragy,** N.M., and Manheimer, W.M.

13a. TYPE OF REPORT	13b. TIME COVERED	14. DATE OF REPORT (Year, Month, Day)	15. PAGE COUNT
Interim	FROM ______ TO ______	1984 December 27	20

16. SUPPLEMENTARY NOTATION

*Laboratory for Plasma and Fusion Energy Studies, Univ. of Maryland, College Park, MD 20742
**Permanent Address: Physics Dept., Univ. of Tanta, Tanta, Egypt

17. COSATI CODES		
FIELD	GROUP	SUB-GROUP

18. SUBJECT TERMS (Continue on reverse if necessary and identify by block number)

Laser fusion , and Energetic electrons ,
Raman sidescatter

19. ABSTRACT (Continue on reverse if necessary and identify by block number)

The theory of the Raman sidescattering instability in an inhomogeneous plasma is revisited. The growth rate is found from the eigenvalue of a second order ordinary differential equation in the Fourier domain. Under certain, rather easily satisfied constraints, the normalized growth rate depends on a single parameter involving laser strength, gradient scale length and resonant density.

20. DISTRIBUTION / AVAILABILITY OF ABSTRACT ☒ UNCLASSIFIED/UNLIMITED ☐ SAME AS RPT ☐ DTIC USERS	21. ABSTRACT SECURITY CLASSIFICATION UNCLASSIFIED
22a. NAME OF RESPONSIBLE INDIVIDUAL Wallace M. Manheimer	22b. TELEPHONE (Include Area Code) (202) 767-3128 — 22c. OFFICE SYMBOL Code 4790

DD FORM 1473, 84 MAR — 83 APR edition may be used until exhausted. All other editions are obsolete.

SECURITY CLASSIFICATION OF THIS PAGE

10. SOURCE OF FUNDING NOS.

PROJECT NO. AI08-79-DP
40092 (172)

CONTENTS

RAMAN SIDESCATTERING IN LASER-PRODUCED PLASMAS

I. Introduction

Raman instabilities, which appear in laser-produced plasmas when the plasma density is less than the quarter-critical density, can lead to hot electron production. These hot electrons could in turn preheat the fuel in laser fusion applications and are therefore a significant concern.[1-3] Of the various Raman instabilities in inhomogeneous plasmas, sidescattering has the lowest threshold and the highest growth rate. Hence, it is a natural focus of theoretical concern.

In this paper, we revisit the theory of this instability. Previous workers[4,5] have determined the threshold to be

$$\left(\frac{V_o}{c}\right)^2 (k_o L)^{4/3} \approx 1, \qquad (1)$$

where V_o is the oscillation velocity in the pump wave field, k_o is the wave number of the pump wave, L is the inhomogeneity scale length, and c is the speed of light. However, the strictly analytical approach of Ref. 4 is not sufficient to determine the accurate numerical value on the right-hand side of Eq. (4). This paper addresses that issue.

The rest of the paper is organized as follows: Section II contains the derivation of our basic equation. In Section III we solve this equation numerically to determine the threshold value. Section IV contains a summary of our principal results.

Manuscript approved September 1984.

II. Derivation of the Raman Sidescattering Equation

Our starting point is the electron fluid equations with the ions serving as a uniform background,

$$\frac{\partial n}{\partial t} + \nabla \cdot n v = 0 \qquad \text{(a)}$$

$$nm \frac{\partial \underline{v}}{\partial t} + nm\underline{v} \cdot \underline{\nabla}\, \underline{v} = -\, 3T\, \underline{\nabla} n - ne\underline{E} - ne \frac{\underline{v}}{c} \times \underline{B} - nm\nu\underline{v} \qquad \text{(b)}$$

$$\underline{\nabla} \cdot \underline{E} = -\, 4\pi\, ne \qquad \text{(c)}$$

$$\underline{\nabla} \cdot \underline{B} = 0 \qquad \text{(d)} \qquad \text{(2)}$$

$$\underline{\nabla} \times \underline{E} = -\frac{1}{c} \frac{\partial \underline{B}}{\partial t} \qquad \text{(e)}$$

$$\underline{\nabla} \times \underline{B} = -\frac{4\pi ne\underline{v}}{c} + \frac{1}{c} \frac{\partial \underline{E}}{\partial t}. \qquad \text{(f)}$$

Since the instability we are considering is parametric, we have the approximate relations

$$\omega_o = \omega_1 + \omega_2$$

$$\underline{k}_o = \underline{k}_1 + \underline{k}_2 \,, \qquad (3)$$

where ω_α and k_α ($\alpha = 0,1,2$) are respectively the frequency and wave number of the incoming pump wave, the outgoing electromagnetic wave, and to the outgoing electrostatic wave. Equation (3) becomes exact in the limit of a homogeneous plasma. Using the homogeneous limit dispersion relations

$$\omega_o^2 = \omega_p^2 + k_o^2\ c^2$$

$$\omega_1^2 = \omega_p^2 + k_1^2\ c^2 \tag{4}$$

$$\omega_2^2 = \omega_p^2 + 3k_2^2\ v_e^2$$

and neglecting V_e^2/c^2, one finds

$$k_1 = (\omega_o^2 - 2\omega_1\omega_p)^{1/2}/c, \tag{5}$$

which confirms that this instability can take place only at densities below quarter-critical.

We chose our coordinates so that the incoming pump wave is polarized in the z-direction and has its wave vector in the x-direction, i.e., $\underset{\sim}{k}_o = k_x\ \hat{\underset{\sim}{e}}_x$. We shall also take $\underset{\sim}{k}_1 = k_y\ \hat{\underset{\sim}{e}}_y - k_z\ \hat{\underset{\sim}{e}}_z$, which is consistent with sidescattering in an arbitrary direction, so that $\underset{\sim}{k}_2 = k_x\ \hat{\underset{\sim}{e}}_x + k_y\ \hat{\underset{\sim}{e}}_y + k_z\ \hat{\underset{\sim}{e}}_z$. We now write

$$\underline{E}_o = \underline{i}_z\ E \exp\ (ik_x\ x-\omega_o t) + c.c.$$

$$\underline{E}_1 = \underline{\varepsilon}(x)\exp\ (-\ ik_y\ y-ik_z z-i\omega_1 t) + c.c. \tag{6}$$

$$\underline{E}_2 = -\ \nabla\phi(x)\exp\ (ik_x x + ik_y y + ik_z z - i\omega_2 t) + c.c.$$

The x-variations of ε and ϕ are due to the inhomogeneity.

To proceed we will use the following ordering. If the dispersion relation for the α mode in the homogeneous system is given by

$D(\omega_\alpha, k_\alpha) = 0$, we assume that in the inhomogeneous system $D(\omega_\alpha, k_\alpha)$, L^{-1}, T_e and nonlinearity are all small, of order δ. Working to lowest order in this quantity δ, we neglect all products of these small quantities.

From Eq. (2b) one finds,

$$\underset{\sim}{V}_o = - \frac{eE_o}{im\omega_1} \tag{7}$$

since the electromagnetic wave has no density perturbation and ν is assumed much less than ω_o.

Turning now to the equation for the electrostatic wave, we find from Eq. (2b)

$$-i\omega_2 \underline{V}_2 + \frac{3T}{m}\frac{\nabla n_2}{n} + \frac{e\underline{E}_2}{m} + \nu_2 V_2 = - \nabla\, (\underline{V}_o \cdot \underline{V}_1{}^*). \tag{8}$$

As is usually the case, the $\underline{V} \cdot \nabla \underline{V}$ nonlinearity cancels the ∇xB nonlinearity. Note also that we now use a subscript 2 on the collision frequency. This (phenomonologically) allows for the fact that the damping of the three different modes may come from different physical processes. For instance to account for Landau damping of the electron plasma wave, ν_2 should be set equal to the collision frequency plus twice the Landau damping rate.

In Eq. (8), $V_1^* = \frac{eE_1^*}{im\omega_1}$, analogous to Eq. (7). From Eq. (2a), we have

$$- i\omega n_2 = - \nabla n_o\, \underline{V}_2, \tag{9}$$

where n_o is the zero-order background density which is x-dependent. We have also assumed that n_o and n_1 equal zero as is appropriate for linear electromagnetic waves. Combining Eqs. (8) and (9) with Poisson's equation, Eq. (4c), we conclude

$$\underline{\nabla}\cdot[\omega_2^2 - \omega_p^2 + 3V_e^2\underline{\nabla}\ \underline{\nabla}\cdot + i\omega_2\nu_2]\ \underline{E}_2 = \frac{\omega_p^2}{\omega_1\omega_2}\frac{e}{m}\nabla^2(\underline{E}_o\cdot\ \underline{E}_1^*), \tag{10}$$

where $V_e^2 = T/m$. In obtaining Eq. (11), we replaced ω_2 with ω_p on the right-hand side.

An analogous derivation yields the equation for the sidescattered wave

$$[\omega_p^2 - \omega_1^2 + i\frac{\nu_1}{\omega_1}\omega_p^2 + c^2\nabla x\nabla x]\underline{E}_1^* = -\frac{e\omega_p}{m\omega_o}[\underline{\nabla}(\underline{E}_o^*\cdot\underline{E}_2) - \underline{E}_o^*\underline{\nabla}\cdot\underline{E}_2]. \tag{11}$$

At this point, we must specify the density inhomogeneity. We shall let

$$\omega_p^2 = \omega_p^{o^2}\ (1 + \frac{x}{L}). \tag{12}$$

The point x = 0 corresponds to the point in the plasma at which the instability which we are considering occurs, ω_p^o is the plasma frequency at that point, and L is the density scale length at that point. Equations (10) and (11) then become

$$\begin{aligned} &\underline{\nabla}\cdot[\omega_2^2 - \omega_p^{o^2} - \omega_p^{o^2}\frac{x}{L} + i\omega_2\nu_2 + 3V_e^2\underline{\nabla}\ \underline{\nabla}\cdot]\underline{E}_2 = \frac{\omega_p^{o^2}}{\omega_1\omega_2}\nabla^2(E_o\cdot E_1^*) \\ &[\omega_p^{o^2}(1 + \frac{x}{L}) - \omega_1^2 + \frac{i\nu}{\omega_1}\omega_p^{o^2} + c^2\underline{\nabla}\times\underline{\nabla}\times]E_1^* = -\frac{e\omega_p}{m\omega_o}[\underline{\nabla}(\underline{E}_o^*\cdot\underline{E}_2) - \underline{E}_o^*\underline{\nabla}\cdot\underline{E}_2]. \end{aligned} \tag{13}$$

We have ignored the x-variation of ω_p^o on the right-hand side of Eq. (13) consistent with our ordering of neglecting products of nonlinearities and ambient gradients.

We further simplify to the case of the scattered wave polarized in the z-direction. Since ponderomotive force goes as $\underline{E}_o \cdot E_1$, this polarization has the largest growth rate, at least in the homogeneous system.

Then the equations can be reduced to

$$\left[2\omega_2\delta\omega + 6iV_e^2k_x\frac{\partial}{\partial x} + 3V_e^2\frac{\partial^2}{\partial x^2} - \omega_p^{o\,2}\frac{x}{L} + i\omega_p^o\nu_2\right]D_2\phi - \frac{\omega_p^{o\,2}}{L}\frac{\partial\phi}{\partial x} = \frac{\omega_p^{o\,2}e}{\omega_o\omega_1 m}E_oD_2\varepsilon_z$$

$$\left[2\omega_1\delta\omega - c^2\frac{\partial^2}{\partial x^2} + \omega_p^{o\,2}\frac{x}{L} + \frac{i\nu_1}{\omega_1}\omega_p^{o\,2}\right]\varepsilon_z = \frac{\omega_1}{\omega_o}\frac{e}{m}E_o^*D_2\phi. \qquad (14)$$

Here we use ϕ, ε_z instead of $\underline{E}_3$, $\underline{E}_z$ as dependent variables. Also

$$D_2 = \frac{\partial^2}{\partial x^2} + 2ik_x\frac{\partial}{\partial x} - k_2^2$$

$$\delta\omega = \delta\omega_1 = -\delta\omega_2, \qquad (15)$$

where $\delta\omega$ is the change in ω from that predicted by the linearized homogeneous dispersion relation. We neglect $(\delta\omega)^2$, and we use $\omega_o = \omega_1 + \omega_2$ to establish $\delta\omega_1 = -\delta\omega_2$. On physical grounds, we expect that the threshold will be lowest in this case, and in the limit $L \to \infty$, $V_e/c \to 0$, we have verified that such is the case. Hence, we focus our attention on Eq. (14).

In solving Eq. (14), it is useful to take the Fourier transform $\begin{pmatrix}\phi(x)\\ \varepsilon(x)\end{pmatrix} = \int_c dk\begin{pmatrix}\phi(K)\\ \varepsilon(K)\end{pmatrix}\exp iKx$. As we will see, $\phi(K)$ and $\varepsilon(K)$ are square integrable and nonsingular along the real K axis so that the contour may be taken as the real K axis. Since upon taking the Fourier transform $\frac{d}{dx} \to iK$ and $x \to i\frac{d}{dK}$, Eq. (14) become two coupled first order equations in the K domain. By standard means, we write them as a single second order equation in in the K domain and eliminate the first derivative term. The result is

$$\frac{d^2\psi}{d\zeta^2} + \left[\gamma + (1-3\frac{V_e^2}{c^2})\zeta^2 - 6\frac{V_e^2}{c^2}\hat{k}_x\zeta\right]^2 - 2i(1-\frac{3V_e^2}{c^2})\zeta + 6i\frac{V_e^2}{c^2}\hat{k}_x^2$$

$$+ \frac{i(k_x + \zeta)}{(\hat{k}_x + \zeta)^2 + \hat{k}_y^2}\left[\gamma + (1 - 3\frac{V_e^2}{c^2})\zeta^2 - 6\frac{V_e^2}{c^2}\hat{k}_x\zeta\right] \tag{16}$$

$$- \frac{1}{4}\frac{\left[3(\hat{k}_x + \zeta)^2 - 2\hat{k}_y^2\right]}{(\hat{k}_x + \zeta)^2 + \hat{k}_y^2} + A\frac{(\hat{k}_x + \zeta)^2 + k_y^2}{\hat{k}_x^2 + \hat{k}_y^2}\quad\psi = 0$$

$$\psi(K) = \varepsilon(K)\exp\frac{iL}{2\omega_p^{o\,2}}\int^K\left[2\omega_2\delta\omega - 6V_e^2k_xK' - 3V_e^2K'^2 + i\omega_p^o\nu_2\right.$$

$$\left. - 2\omega_1\delta\omega + K'^2c^2 + i\frac{\omega_p^{o\,2}}{\omega_1}\nu_1 - \frac{k_x + K'}{(k_x + K')^2 + k_y^2}\right]dK^1. \tag{17}$$

Also

$$\gamma = \left[2\omega_o\delta\omega + i\omega_p^o(\nu_2 + \frac{\omega_p^o}{\omega_1}\nu_1)\right]\frac{X^2_{int}}{c^2}$$

$$X_{int} = (Lc^2/2\omega_p^{o\,2})^{1/3},\ \hat{k}_{x,y} = k_{x,y}X_{int},\ \zeta = KX_{int} \tag{18}$$

$$A = 4\frac{\omega_p^{o\,2}}{\omega_1^2}\left|\frac{eE_o}{mc^2}\right|^2 k_2^2\,X^4_{int} \equiv \frac{\omega_{po}^2\,V_{os}^2\,k_2^2\,X^4_{int}}{c^4},\ V_{os} = \frac{2eE_o}{m\omega_o}.$$

The quantity k_2 is the magnitude of the wave number of the plasma wave in the honogeneous system, $c^2k_2^2 = 2\omega_o^2 - 2\omega_o\omega_p^o - \omega_p^{o\,2}$. Finally, letting $V_e^2/c^2 \to 0$, and then letting $\hat{k}_x \to \infty$, Eq. (16) reduces to

$$\frac{d^2\psi}{d\zeta^2} + [(\gamma + \zeta^2)^2 - 2i\zeta + A]\psi = 0. \qquad (19)$$

Not only is Eq. (19) much simpler than Eq. (16), but also the dimensionality of the parameter space has been substantially reduced. Now γ depends only on the single parameter A, whereas in Eq. (16) it depended on A, v_e/c, $\hat{k}_x$ and $\hat{k}_y$. We will show that for parameters of the NRL[6] experiment, the approximations in deriving Eq. (19) are very well satisifed.

III. Determination of the Raman Sidescattering Threshold

At threshold, all the terms in Eq. (19) must roughly balance. It follows that $A \sim 1$, or, letting $v_o^2 = 4e^2|\varepsilon^2|/m^2\omega_1^2$, we find

$$\frac{v_{os}^2\, k_2^2\, (k_1 L)^{4/3}}{2^{4/3}\, \omega_p^{o\,2} \left(\frac{\omega_p^2}{\omega_p^{o2}} - 1\right)^{2/3}} \sim 1. \qquad (20)$$

Equation (20) is essentially the same as Eq. (1) near quarter-critical density. When $A >> 1$, then the only way to balance the term $A\psi$ is by requiring that $\gamma^2 + A = 0$. We then find

$$\gamma = iA^{1/2}, \qquad (21)$$

for the growth rate. It is interesting to note that the limit $A \to \infty$ does not correspond to the homogeneous limit at $x = 0$ as one might naively expect, but rather at $x = (L/\omega_{po}^2)\,[2\omega_2\delta\omega + i\omega_p^o \nu_2 - 2\omega_1\delta\omega - i\nu_1(\omega_p^{o2}/\omega_2)]$. It is possible to refine[4] the estimates in Eqs. (20) and (21) but an exact solution of Eqs. (16) and (19) requires a numerical approach.

We begin by specifying the appropriate boundary conditions for E

Asymptotically, as ζ goes to $\pm\infty$, we have

$$\psi \sim \exp\left[\pm i(\zeta^3/3 + \gamma\zeta)\right]. \qquad ($$

As a consequence of causality, we demand that the solution decay along real ζ-axis when $\mathrm{Im}(\gamma) > 0$. It follows that we want the positive solu when $\zeta \to +\infty$ and the negative solution when $\zeta \to -\infty$.

To determine the eigenvalues of Eq. (19), we calculate the determ the solution matrix $D(\gamma)$ using a finite-element code.[7] The roots of t determinant $D(\gamma)$ correspond to the eigenvalues. We began by finding a roots of $D(\gamma)$ in a fairly sizeable box in the complex γ-plane ($-6.0 \leq \mathrm{Re}(\gamma) \leq 6.0$, $-4.0 \leq \mathrm{Im}(\gamma) \leq 4.5$) with A set equal to 1. To we use Nyquist's theorem

$$N = \frac{1}{2\pi i} \int_c \frac{d|D(\gamma)|}{D(\gamma)}, \qquad ($$

to calculate the number of roots N in the box. By repeated quadrasect determine smaller boxes in which only a single root lies. The root lo γ_o is then estimated using the relation

$$\gamma_o = \frac{1}{2\pi i} \int_c \frac{\gamma\, d|D(\gamma)|}{D(\gamma)}. \qquad ($$

The exact root location is then homed-in on using a secant-grid algori This Nyquist algorithm is optimized in a number of respects and runs fa rapidly. (For the case just described, the program made roughly 35,00 determinations of $D(\gamma)$ and took roughly 13 minutes of c.p.u. time to ru CDC 7600.)

It should be stressed that the eigenmodes corresponding to eigenvalues with $Im(\gamma) < 0$ are unphysical since they correspond to modes which grow along the real ζ-axis as $\zeta \to \pm \infty$, so that their Fourier transforms do not exist. The eigenvalues for the five unstable modes which the routine found are given in Table I for the case $A = 1$. The number of significant figures was determined by increasing the width of the integration region and doubling the number of modes; those figures which did not change were deemed significant and included in the table. The critical value of A at which $Im(\gamma) = 0$, A_{crit}, was then found for each of the five most unstable modes by following the eigenvalues parametrically as A was reduced. The results are shown in Table II, the overall marginally stability point is given by $A = 0.37$. We then repeated the calculation using Eq. (16) rather than Eq. (19) with $\hat{k}_x = 10$, $\hat{k}_y = 0$ corresponding to quarter critical density and $V_e^2/c^2 = 0.0013$. These values correspond to those in the NRL long scale length experiment. Results are also shown in Table II. There is evidently good agreement between the results using Eq. (16) and the results using Eq. (19).

In Fig. 1 is shown a plot of the growth rate versus A for the most unstable mode, determined from a numerical solution of Eq. (19). In physical units

$$\left[2\omega_o \delta\omega + i\omega_{po}(\nu_2 + \frac{\omega_p^o}{\omega_1} \nu_1)\right] \frac{X_{int}^2}{c^2} = i\gamma(A), \qquad (25)$$

where $\gamma(A)$ is defined graphically in Fig. 1, and A and X_{int} are defined in Eqs. (18). A recent analytic theory[8] also shows that the growth rate depends on the single parameter A. In Ref. 8, it can be shown that their expression for growth rate reduces to $\gamma = A^{1/2}[1 - 0.5\ A^{-3/2}]$ so that the threshold is given by $A = 0.63$. Thus the analytic theory predicts a threshold higher by almost a factor of two.

Table I The real and imaginary parts of γ (positive imaginary part means growth) for A = 1 for the 5 unstable modes. The eigenvalues are calculated from Eq. (16) and also from Eq. (19) with $\hat{k}_x = 10$, $\hat{k}_y = 0$, $3\ V_e^2/c^2 = 0.00013$.

Mode Number	Re γ, Imγ, Eq. (19)	Reγ, Imγ, Eq. (16)
1	−0.4564, 0.5091	−0.4597 0.5168
2	−1.794, 0.1418	−1.789 0.1473
3	−2.835, 0.06217	−2.827 0.06516
4	−3.7114, 0.0289	−3.7020 0.0304
5	−4.49, 0010	−4.48 0.011

Table II The value of $A \equiv A_{(crit)}$ for marginal stability for the 5 unstable modes.

Mode Number	$A_{(crit)}$, Eq. (19)	$A_{(crit)}$, Eq. (16)
1	0.37485	0.36762
2	0.6188	0.6102
3	0.7567	0.7498
4	0.858	0.854
5	0.9	0.9

In practice, an important effect is tranverse convection across the finite spot size. This is an extremely complicated process.[9] The theory of Liu, et al.[4] indicates that the growth rate must be larger than the convection time, or $\mathrm{Im}\,\delta\omega > V_g/L_T$ where L_T is the transverse scale length. If $V_g = c$, (as it is at densities less than about one-eighth critical) a 100 μ spot size means the growth rate must be larger than about $3 \times 10^{12}\mathrm{sec}^{-1}$, a fairly sizeable requirement on $\mathrm{Im}\,\delta\omega$. However at the quarter-critical density the transverse scattered photon velocity vanishes so that here the condition disappears.

From Eq. (25), we conclude that the instability threshold is given by $\mathrm{Im}\,[\gamma(A)] = \omega_{po}[\nu_2 + (\omega_p^o/\omega_o)\nu_1]\,(X_{int}^2/c^2)$ rather than $\mathrm{Im}\,[\gamma(A)] = 0$. In this expression, the ν's are the electron ion momentum collision frequency plus twice any damping rate of the wave. For the electron plasma wave ν_2 must also include the Landau damping. The phase velocity of the wave is given by ω_{po}/k_2. We have verified that Landau damping plays a negligible role for NRL parameters (Te = 600 e.v.) for densities larger than one-tenth the quarter-critical density. By contrast, the collisions make a significant contribution to the threshold in density. In the NRL long scale length experiment,[5] $L = 140\mu$, $Z \sim 5$, $T_e \sim 600$ eV. Thus at the quarter-critical density, taking into account collision damping, the threshold for Raman sidescatter is $A = 0.46$ or $I = 1.6 \times 10^{14}\,\mathrm{w/cm}^2$ using the fact that $V_{os} = 25.6\, I^{1/2}(\mathrm{w/cm}^2)\,\lambda_o(\mu)$.

IV. Summary

In this paper we have revisited the theory of Raman sidescattering in laser produced plasmas. We have shown that to a very good approximation the growth rate and thresholds can be reduced to examining a single parameter system. We find that at quarter-critical density, the threshold for stimulated Raman sidescatter in the NRL long scale length experiment is given roughly by $I \geq 1.6 \times 10^{14} \omega/cm^2$.

Acknowledgments

The authors gratefully acknowledge useful conversations with Dr. T. M. Antonsen, Dr. J. M. Finn, and Dr. P. N. Guzdar. This work has been supported by the Department of Energy and the Naval Research Laboratory. Additionally, one of us (N. M. El-S.*) has been supported by the Binational Fulbright Commission, and he would like to thank Professor E. Ott for his hospitality while at the University of Maryland.

*Permanent Address: Physics Department, Faculty of Science, University of Tanta, Tanta, Egypt.

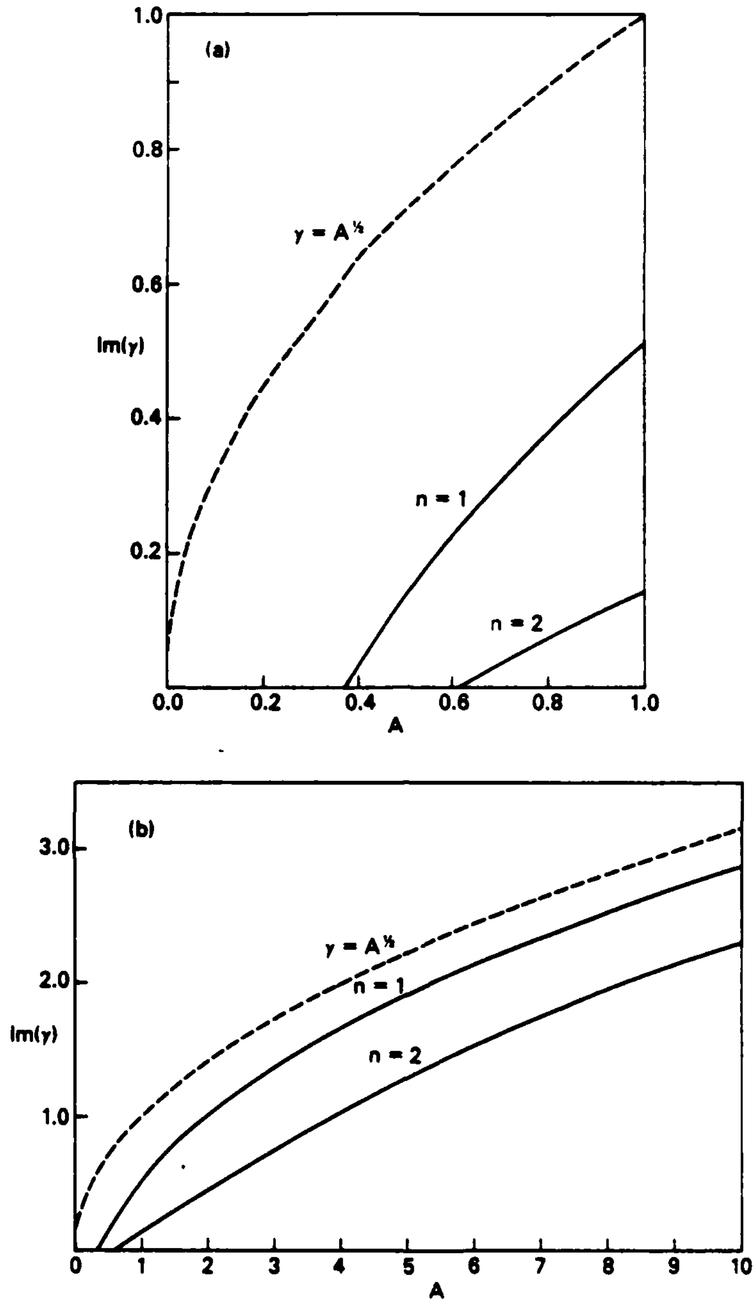

Fig. 1 The imaginary part of γ as a function of A for the two fastest growing modes. a) Detailed plot for $0 < A < 1$, b) plot for $0 < A < 10$.

References

1. W. L. Kruer, "Theory and Simulation of Laser Plasma Coupling", (20th Scottish University Summer School, St. Andrews, Scotland, 1979); W. L. Kruer, "Theory and Simulation of Laser Plasma Coupling-II", (24th Scottish University Summer School, St. Andrews, Scotland, 1982).

2. C. E. Max, "Physics of the Coronal Plasma", in Laser Fusion Targets in Laser-Plasma Interaction, ed. by R. Balian and J.-C. Adam (North-Holland, New York, 1982).

3. W. L. Kruer, Comments Plasma Phys. Controlled Fusion 7, 215 (1983).

4. C. S. Liu, M. N. Rosenbluth and R. B. White, Phys. Fluids 17, 1211 (1974).

5. H. H. Klein, W. M. Manheimer and E. Ott, Phys. Rev. Lett. 31, 1187 (1973).

6. M. J. Herbst, J. Grun, J. Gardner, J. A. Stamper, F. C. Young, S. P. Obenschain, E. E. McLean and B. H. Ripin, Phys. Rev. Lett. 52, 192 (1984); see also F. C. Young, M. J. Herbst, J. H. Gardner, K. J. Kearney, J. A. Stamper, S. P. Obenschain, J. Grun, E. A. McLean and B. H. Ripin, NRL Memorandum Report 5174, "X-Ray Production in Long-Scalelength Laser-Plasma Interaction Experiments."

7. W. Miner, Ph.D Thesis (University of Texas at Austin, unpublished, 1979).

8. B. Afeyan and E. Williams, Phys. Fluids, to be published.

9. M. A. Mostrom and A. N. Kaufman, Phys. Rev. Lett. 42, 644 (1979).

END

FILMED

1-85

DTIC

CDC 7600